Available online at http://scik.org
Commun. Math. Biol. Neurosci. 2024, 2024:11
https://doi.org/10.28919/cmbn/8313
ISSN: 2052-2541

STABILITY AND BIFURCATION ANALYSIS OF A DISCRETE PREDATOR-PREY SYSTEM OF RICKER TYPE WITH HARVESTING EFFECT

M. IMRAN[1], M. B. ALMATRAFI[2,*], R. AHMED[1]

[1]Department of Mathematics, Air University Multan Campus, Multan, Pakistan

[2]Department of Mathematics, College of Science, Taibah University, Al-Madinah Al-Munawarah, Saudi Arabia

Abstract. In ecosystems, the harvesting effect is crucial for maintaining predator-prey relationships. The goal of this study is to look into the complexity of a discrete-time predator-prey system with a harvesting effect. The occurrence and stability of fixed points, as well as period-doubling and Neimark-Sacker bifurcations, are all investigated in this study. The system's bifurcating and fluctuating behavior can be controlled via feedback and hybrid control approaches. Furthermore, numerical simulations are employed as evidence to support our theoretical findings. It has been discovered that the harvesting effect can have a major impact on the dynamics of the predator-prey system. The predator and prey populations can benefit or be harmed depending on the intensity of harvesting.

Keywords: predator-prey; Ricker; harvesting; stability; bifurcation; chaos control.

2020 AMS Subject Classification: 39A28, 39A30, 92D25.

1. Introduction

The relationship between predators and their prey has been an integral subject in the fields of ecology and mathematical ecology, owing to its widespread occurrence and significance. Efforts have been made to comprehend and elucidate predator-prey interactions via the development and analysis of mathematical systems. Lotka [1] and Volterra [2] devised a foundational

*Corresponding author

E-mail address: mmutrafi@taibahu.edu.sa

Received November 01, 2023

predator-prey system including two species. Over the course of time, numerous scholars have made improvements to this particular system with the intention of providing a more accurate explanation and improving understanding. This is due to its shortcomings in fitting various real-life situations and complexities [3, 4, 5, 6, 7, 8].

Several studies have employed the logistic map as a tool to demonstrate the growth of prey species [9, 10, 11, 12]. However, a dearth of scholarly investigations exists regarding the stability analysis of a discrete predator-prey system that integrates prey growth via a Ricker map [13, 14, 15]. The Ricker map exhibits a population growth pattern that can be approximated as exponential in nature. Nevertheless, it is observed that as the population size expands, the rate of population growth tends to decline. Over time, the population stabilizes at a plateau and demonstrates variations around an average value.

The functional response is a crucial factor in the population dynamics of predator-prey interactions. A functional response refers to the quantification of the consumption rate of prey per predator. There are various kinds of functional responses that have been identified in the literature. These include Holling I-III [16], ratio-dependent [17], Beddington-DeAngelis [18, 19], Crowley-Martin [20], and square root [21].

When considering the modeling of dynamical systems, it is customary for such systems to be shown in one of two manners: i) as continuous-time systems, which are characterized by differential equations, or ii) as discrete-time systems, which are characterized by difference equations. Over the course of time, researchers have undertaken comprehensive inquiries into the nonlinear dynamic characteristics displayed by continuous systems. In recent times, there has been a notable surge in the scholarly interest in discrete-time systems, as evidenced by the considerable attention given by many scholars [22, 23, 24, 25]. This is due to the fact that discrete systems exhibit greater efficiency in non-overlapping generation compared to continuous systems. One of the benefits of discrete-time systems is their ability to facilitate the acquisition of numerical solutions. Moreover, a massive number of studies indicates that discrete-time systems may exhibit more complicated dynamics compared to their continuous-time counterparts [26, 27, 28, 29, 30, 31, 32, 33]. Therefore, discrete systems possess more attraction in comparison to continuous systems.

There exist two distinct techniques for acquiring a discrete system. One approach is initially examining a continuous system and subsequently transforming it into a discrete system by the utilization of several techniques, including the Euler technique [34, 35, 36, 37, 38] and the piecewise constant argument method [39, 40, 41, 42]. Conversely, we initiate the study directly by considering the discrete system. Hamada et al. [43] investigated the following discrete predator-prey system that incorporates a Ricker type growth function:

$$(1)\qquad \begin{cases} x_{n+1} = rx_n e^{1-x_n} - \frac{bx_n^2 y_n}{1+x_n^2}, \\ y_{n+1} = \frac{bx_n^2 y_n}{1+x_n^2}, \end{cases}$$

where x_n represents the density of prey, y_n is the density of predators, $r > 0$ indicates the rate at which the prey population rises, and $b > 0$ represents the maximum value that the prey's per capita drop rate may attain.

The influence of harvesting on the dynamics of a predator-prey system is widely acknowledged. The primary objective of a harvesting system is to ascertain the maximum harvestable quantity while avoiding significant detrimental impacts on the population being harvested. Population harvesting is a prevalent practice in the fields of forestry, fishing, and wildlife management. Over the past few years, various methods of harvesting have been developed and examined, including constant harvesting, proportional harvesting, and nonlinear harvesting. The impact of harvesting on the dynamics of predator-prey systems has been extensively studied in a number of scholarly works [44, 45, 46, 47, 48, 49, 50, 51, 52, 53, 54, 55, 56, 57, 58].

As a result of the preceding discussion, we naturally need to know: what happens to the dynamical properties when a harvesting effect is added to the prey population in system (1)? As a result, we extend system (1) by including a harvesting effect on the prey population. As a result, the modified system is given as follows:

$$(2)\qquad \begin{cases} x_{n+1} = rx_n e^{1-x_n} - \frac{bx_n^2 y_n}{1+x_n^2} - hx_n, \\ y_{n+1} = \frac{bx_n^2 y_n}{1+x_n^2}, \end{cases}$$

where h is the harvesting rate.

The subsequent sections of the paper are structured in the following manner: The focus of Section 2 is to examine the existence and topological categorization of fixed points. Section

3 delves into the bifurcation analysis of the period-doubling (PD) and Neimark-Sacker (NS) phenomena at the positive fixed point. Section 4 employs two control methodologies in order to effectively regulate bifurcations and chaos. In order to validate and explicate the theoretical findings, numerical examples are presented in Section 5. Finally, the analysis conducted in this study is summarized in Section 6.

2. TOPOLGICAL CLASSIFICATION OF FIXED POINTS

The understanding the stability of the fixed points holds significant importance within the context of a predator-prey system. The fixed points represent equilibrium states wherein the populations of predators and prey have achieved a condition of balance. By conducting an analysis of their stability, we are able to make predictions about the long-term patterns exhibited by these ecological systems, gaining a deeper understanding of the various factors that contribute to the overall dynamics of the ecosystem.

2.1. Existence of Fixed Points.

The fixed points for system (2) can be obtained by solving the following system:

$$\begin{cases} x = rxe^{1-x} - \frac{bx^2y}{1+x^2} - hx, \\ y = \frac{bx^2y}{1+x^2}, \end{cases} \tag{3}$$

for x and y. It is obtained that system (2) has three fixed points $E_0 = (0,0), E_1 = (1 + ln(\frac{r}{1+h}), 0)$ and

$$E_2 = \left(\frac{1}{\sqrt{b-1}}, \frac{-1-h+re^{1-\frac{1}{\sqrt{b-1}}}}{\sqrt{b-1}} \right).$$

The trivial fixed point $E_0 = (0,0)$ always exists. The predator-free fixed point $E_1 = (1 + ln(\frac{r}{1+h}), 0)$ exists if $r > \frac{1+h}{e}$. The coexistence fixed point $E_2 = \left(\frac{1}{\sqrt{b-1}}, \frac{-1-h+re^{1-\frac{1}{\sqrt{b-1}}}}{\sqrt{b-1}} \right)$ exists if $b > 1$ and $r > (1+h)e^{-1+\frac{1}{\sqrt{b-1}}}$.

2.2. Stability of Fixed Points.

To classify the fixed points, we employ the following results.

Lemma 2.1. [59] *Let $\Lambda(\xi) = \xi^2 + K_1\xi + K_0$ be the characteristic polynomial of Jacobian matrix computed at fixed point (x,y) and ξ_1, ξ_2 satisfy $\Lambda(\xi) = 0$, then (x,y) is a*

(1) sink (locally asymptotically stable (LAS)) when $|\xi_1| < 1$ along with $|\xi_2| < 1$,

(2) source when $|\xi_1| > 1$ *along with* $|\xi_2| > 1$*,*

(3) saddle point (SP) when $|\xi_1| < 1 \wedge |\xi_2| > 1$ *(or* $|\xi_1| > 1 \wedge |\xi_2| < 1$*),*

(4) non-hyperbolic point (NHP) when the absolute value of either of ξ_1 *and* ξ_2 *is one.*

Lemma 2.2. [59]

Consider the quadratic function $\Lambda(\xi) = \xi^2 + K_1\xi + K_0$*. Suppose that* $\Lambda(1) > 0$*. If* ξ_1 *and* ξ_2 *both satisfy the equation* $\Lambda(\xi) = 0$*, then*

(1) $|\xi_1| < 1$ *along with* $|\xi_2| < 1$ *if* $\Lambda(-1) > 0 \wedge K_0 < 1$*,*

(2) $|\xi_1| < 1 \wedge |\xi_2| > 1$ *(or* $|\xi_1| > 1 \wedge |\xi_2| < 1$*) if* $\Lambda(-1) < 0$*,*

(3) $|\xi_{1,2}| > 1$ *if* $\Lambda(-1) > 0 \wedge K_0 > 1$*,*

(4) $|\xi_2| \neq 1 \wedge \xi_1 = -1$ *if* $\Lambda(-1) = 0 \wedge K_1 \neq 0, 2$*,*

(5) $\xi_1, \xi_2 \in \mathbb{C}$ *along with* $|\xi_{1,2}| = 1$ *if* $K_1^2 - 4K_0 < 0 \wedge K_0 = 1$*.*

Through simple computations, one can obtain the Jacobian matrix at an arbitrary fixed point (x,y) as follows:

$$J(x,y) = \begin{bmatrix} -e^{1-x}r(-1+x) - \frac{h(1+x^2)^2+2bxy}{(1+x^2)^2} & -\frac{bx^2}{1+x^2} \\ \frac{2bxy}{(1+x^2)^2} & \frac{bx^2}{1+x^2} \end{bmatrix}.$$

The Jacobian matrix of system (2) computed at E_0 is shown as follows:

$$J(E_0) = \begin{bmatrix} -h+er & 0 \\ 0 & 0 \end{bmatrix}.$$

Also, the Jacobian matrix at E_1 is given by

$$J(E_1) = \begin{bmatrix} -h-(1+h)ln(\frac{r}{1+h}) & -\frac{b(1+ln(\frac{r}{1+h}))^2}{1+(1+ln(\frac{r}{1+h}))^2} \\ 0 & \frac{b(1+ln(\frac{r}{1+h}))^2}{1+(1+ln(\frac{r}{1+h}))^2} \end{bmatrix}.$$

Proposition 2.3. *The trivial fixed point* E_0 *is a*

(1) LAS if any one of the following conditions satisfies:

(i) $0 < h \leq 1$ *and* $0 < r < \frac{1+h}{e}$*,*

(ii) $h > 1$ *and* $\frac{-1+h}{e} < r < \frac{1+h}{e}$*,*

(2) SP if any one of the following conditions satisfies:

(i) $0 < h \leq 1$ *and* $r > \frac{1+h}{e}$*,*

(ii) $h > 1$ *and* $0 < r < \frac{-1+h}{e}$,

(iii) $h > 1$ *and* $r > \frac{1+h}{e}$,

(3) NHP if any one of the following conditions satisfies:

(i) $0 < h \leq 1$ *and* $r = \frac{1+h}{e}$,

(ii) $h > 1$ *and* $r = \frac{-1+h}{e}$,

(iii) $h > 1$ *and* $r = \frac{1+h}{e}$.

Proposition 2.4. *Assume that* $\omega_1 = e^{-1+\frac{1}{\sqrt{b-1}}}(1+h)$ *and* $\omega_2 = e^{\frac{1-h}{1+h}}(1+h)$. *The fixed point* E_1 *is*

(1) LAS if any one of the following conditions satisfies:

(i) $0 < b \leq 1$ *and* $\frac{1+h}{e} < r < \omega_2$,

(ii) $b > 1$ *and* $\frac{1+h}{e} < r < min\{\omega_1, \omega_2\}$,

(2) source if $b > 1$ *and* $r > \max\{\omega_1, \omega_2\}$,

(3) SP if any one of the following conditions satisfies:

(i) $0 < b \leq 1$ *and* $r > \max\{\frac{1+h}{e}, \omega_2\}$,

(ii) $b > 1$ *and* $max\{\frac{1+h}{e}, \omega_2\} < r < \omega_1$,

(iii) $b > 1$ *and* $max\{\frac{1+h}{e}, \omega_1\} < r < \omega_2$,

(4) NHP if any one of the following conditions satisfies:

(i) $b > 1$ *and* $r = \omega_1$,

(ii) $r = \omega_2$.

Next, we classify the positive fixed point E_2 of system (2) according to the above Jacobian matrix and Lemma 2.2. We obtain

$$J(E_2) = \begin{bmatrix} a_{11} & -1 \\ a_{21} & 1 \end{bmatrix}, \tag{4}$$

where

$$a_{11} = \frac{-2-2h+2e^{1-\frac{1}{\sqrt{-1+b}}}r + b(2+h+(-1-\frac{1}{\sqrt{-1+b}})e^{1-\frac{1}{\sqrt{-1+b}}}r)}{b},$$

$$a_{21} = \frac{2(-1+b)(-1-h+e^{1-\frac{1}{\sqrt{-1+b}}}r)}{b}.$$

The characteristic polynomial of $J(E_2)$ is

$$\Lambda(\xi) = \xi^2 + K_1\xi + K_0,$$

where

$$K_1 = \frac{2+2h-2e^{1-\frac{1}{\sqrt{-1+b}}}r + b(-3-h+(1+\frac{1}{\sqrt{-1+b}})e^{1-\frac{1}{\sqrt{-1+b}}}r)}{b},$$
$$K_0 = -h + \frac{(-1+\sqrt{-1+b})e^{1-\frac{1}{\sqrt{-1+b}}}r}{\sqrt{-1+b}}.$$

It can be obtained through calculations that

$$\Lambda(0) = -h + \frac{(-1+\sqrt{-1+b})e^{1-\frac{1}{\sqrt{-1+b}}}r}{\sqrt{-1+b}},$$
$$\Lambda(-1) = -\frac{2(1+h-e^{1-\frac{1}{\sqrt{-1+b}}}r + b(-2+\frac{e^{1-\frac{1}{\sqrt{-1+b}}}r}{\sqrt{-1+b}}))}{b},$$
$$\Lambda(1) = \frac{2(-1+b)(-1-h+e^{1-\frac{1}{\sqrt{-1+b}}}r)}{b}.$$

Theorem 2.5. *Assume that* $h_1 = re^{1-\frac{1}{\sqrt{-1+b}}} - b(-2+\frac{e^{1-\frac{1}{\sqrt{-1+b}}}r}{\sqrt{-1+b}}) - 1$ *and* $h_2 = \frac{r(-1+\sqrt{-1+b})e^{1-\frac{1}{\sqrt{-1+b}}}}{\sqrt{-1+b}} - 1$. *The positive fixed point*

(1) E_2 *is LAS if* $h_2 < h < h_1$,

(2) E_2 *is a source if* $h < min\{h_1, h_2\}$,

(3) E_2 *is a SP if* $h > h_1$,

(4) E_2 *is NHP and experiences PD bifurcation if* $h = h_1$ *and*

$$r \neq \frac{2\sqrt{b-1}}{e^{1-\frac{1}{\sqrt{-1+b}}}}, \frac{2b}{\sqrt{b-1}e^{1-\frac{1}{\sqrt{-1+b}}}},$$

(5) E_2 *is NHP and experiences NS bifurcation if* $h = h_2$ *and*

$$\frac{b-2}{2\sqrt{b-1}e^{1-\frac{1}{\sqrt{-1+b}}}} < r < \frac{5b-2}{2\sqrt{b-1}e^{1-\frac{1}{\sqrt{-1+b}}}}.$$

3. BIFURCATION ANALYSIS

This section is focused on conducting a comprehensive investigation of the bifurcation phenomenon involving PD and NS bifurcation in system (2) at the positive fixed point E_2. In order to obtain a thorough treatment of bifurcation analysis, we recommend that readers refer to [60, 61]. The bifurcation holds significant implications for the dynamics of the system, shedding light on scenarios where even slight modifications to parameters yield substantial alterations in the dynamics of predator-prey relationships. In addition, gaining knowledge about PD and NS bifurcations contributes to a deeper comprehension of ecosystem dynamics. This understanding, in turn, facilitates the formulation of effective conservation and management strategies aimed at sustaining the enduring coexistence of predator and prey populations. This study initiates by investigating the PD bifurcation at E_2 based on condition (4) as presented in Theorem 2.5. By applying a small perturbation δ ($|\delta| \lll 1$) to the bifurcation parameter around the critical value h_1, system (2) is changed to

$$\begin{cases} x_{n+1} = rx_n e^{1-x_n} - \frac{bx_n^2 y_n}{1+x_n^2} - (h+\delta)x_n, \\ y_{n+1} = \frac{bx_n^2 y_n}{1+x_n^2}. \end{cases} \tag{5}$$

We transform the fixed point E_2 to the origin by considering the change of variables $u_n = x_n - \frac{1}{\sqrt{b-1}}$, $v_n = y_n - \frac{-1-h+re^{1-\frac{1}{\sqrt{b-1}}}}{\sqrt{b-1}}$. After substituting $h = h_1$, system (5) is transformed into the following form:

$$\begin{bmatrix} u_{n+1} \\ v_{n+1} \end{bmatrix} = \begin{bmatrix} -3+2b-\sqrt{-1+b}e^{1-\frac{1}{\sqrt{-1+b}}}r & -1 \\ 4-4b+2\sqrt{-1+b}e^{1-\frac{1}{\sqrt{-1+b}}}r & 1 \end{bmatrix} \begin{bmatrix} u_n \\ v_n \end{bmatrix} + \begin{bmatrix} F(u_n,v_n,\delta) \\ G(u_n,v_n,\delta) \end{bmatrix}, \tag{6}$$

where

$$F(u_n,v_n,\delta) = a_1u_n^2 + a_2u_n^3 + a_3u_nv_n + a_4u_n^2v_n + a_5u_n\delta + a_6u_n^2\delta + O((|u_n|+|v_n|+|\delta|)^4),$$

$$G(u_n,v_n,\delta) = b_1u_n^2 + b_2u_n^3 + b_3u_nv_n + b_4u_n^2v_n + b_5u_n\delta + b_6u_n^2\delta + O((|u_n|+|v_n|+|\delta|)^4),$$

$$a_1 = \frac{4(-4+b)(-1+b)^{3/2} + \frac{(8+(-16+\sqrt{-1+b})b+10b^2-2b^3)e^{1-\frac{1}{\sqrt{-1+b}}}r}{-1+b}}{2b},$$

$$a_2 = \frac{-48(-2+b)(-1+b)^2 + \frac{(-48+120b+(-97+3\sqrt{-1+b})b^2+24b^3)e^{1-\frac{1}{\sqrt{-1+b}}}r}{\sqrt{-1+b}}}{6b^2},$$

$$a_3 = -\frac{2(-1+b)^{3/2}}{b},$$
$$a_4 = -\frac{(-4+b)(-1+b)^2}{b^2},$$
$$a_5 = \frac{(-2+b)}{b},$$
$$a_6 = \frac{(-4+b)(-1+b)^{3/2}}{b^2},$$
$$b_1 = -\frac{(-4+b)(-1+b)e^{-\frac{1}{\sqrt{-1+b}}}(2\sqrt{-1+b}e^{\frac{1}{\sqrt{-1+b}}} - er)}{b},$$
$$b_2 = \frac{4(-2+b)(-1+b)^{3/2}e^{-\frac{1}{\sqrt{-1+b}}}(2\sqrt{-1+b}e^{\frac{1}{\sqrt{-1+b}}} - er)}{b^2},$$
$$b_3 = \frac{2(-1+b)^{3/2}}{b},$$
$$b_4 = \frac{(-4+b)(-1+b)^2}{b^2},$$
$$b_5 = -2+\frac{2}{b},$$
$$b_6 = -\frac{(-4+b)(-1+b)^{3/2}}{b^2}.$$

Next, system (6) is diagonalized through the consideration of the following transformation:

$$\begin{bmatrix} u_n \\ v_n \end{bmatrix} = \begin{bmatrix} \frac{e^{\frac{1}{\sqrt{-1+b}}}}{-2e^{\frac{1}{\sqrt{-1+b}}}+2be^{\frac{1}{\sqrt{-1+b}}}-\sqrt{-1+b}er} & -\frac{1}{2} \\ 1 & 1 \end{bmatrix} \begin{bmatrix} X_n \\ Y_n \end{bmatrix}, \tag{7}$$

Upon applying the mapping (7), the system (6) undergoes the alteration as follows:

$$\begin{bmatrix} X_{n+1} \\ Y_{n+1} \end{bmatrix} = \begin{bmatrix} -1 & 0 \\ 0 & \xi \end{bmatrix} \begin{bmatrix} X_n \\ Y_n \end{bmatrix} + \begin{bmatrix} \Gamma(X_n, Y_n, \delta) \\ \Upsilon(X_n, Y_n, \delta) \end{bmatrix}, \tag{8}$$

where

$$\xi = -1+2b-\sqrt{-1+b}e^{1-\frac{1}{\sqrt{-1+b}}}r,$$

$$\Gamma(X_n,Y_n,\delta) = c_1X_nY_n + c_2Y_n^3 + c_3Y_n^2 + c_4X_n^2 + c_5X_n^3 + c_6X_n^2Y_n + c_7X_nY_n^2 + c_8Y_n\delta$$
$$+ c_9X_nY_n\delta + c_{10}X_n^2\delta + c_{11}Y_n^2\delta + c_{12}X_n\delta + O((|X_n|+|Y_n|+|\delta|)^4),$$
$$\Upsilon(X_n,Y_n,\delta) = d_1X_nY_n + d_2Y_n^2 + d_3X_n^2 + d_4Y_n^3 + d_5X_nY_n^2 + d_6X_n^2Y_n + d_7X_n^3 + d_8Y_n^2\delta$$

$$+d_9X_n^2\delta+d_{10}X_nY_n\delta+d_{11}Y_n\delta+d_{12}X_n\delta+O((|X_n|+|Y_n|+|\delta|)^4),$$

where the values of coefficients are given in Appendix A. Next, assume that Q^C be the center manifold of (8) intended at origin in a close neighborhood of $\delta=0$. It can be approximated as follows:

$$Q^C=\left\{(X_n,Y_n,\delta)\in\mathbb{R}^3_+\middle|Y_n=p_1X_n^2+p_2X_n\delta+p_3\delta^2+O((|X_n|+|\delta|)^3)\right\},$$

where

$$p_1=\frac{d_3}{1-\xi},\ p_2=-\frac{d_{12}}{1+\xi},\ p_3=0.$$

As a result, system (8) is limited to Q^C in the manner as follows:

$$\tilde{F}:=e_{n+1}=-X_n+c_4X_n^2+c_{12}X_n\delta+\left(c_5-\frac{c_1d_3}{-1+\xi}\right)X_n^3+\left(c_{10}-\frac{c_8d_3}{-1+\xi}-\frac{c_1d_{12}}{1+\xi}\right)X_n^2\delta$$

$$-\frac{c_8d_{12}}{1+\xi}X_n\delta^2+O\left((|X_n|+|\delta|)^4\right). \tag{9}$$

For the function (9) to go through PD bifurcation, it is necessary that the following two quantities possesses non-zero values:

$$l_1=\tilde{F}_\delta\tilde{F}_{X_nX_n}+2\tilde{F}_{X_n\delta}\bigg|_{(0,0)}=2c_{12}, \tag{10}$$

$$l_2=\frac{1}{2}(\tilde{F}_{X_nX_n})^2+\frac{1}{3}\tilde{F}_{X_nX_nX_n}\bigg|_{(0,0)}=2\left(c_4^2+c_5-\frac{c_1d_3}{-1+\xi}\right). \tag{11}$$

From the previous discussion, we get the following theorem:

Theorem 3.1. *Assume that condition (4) of Theorem 2.5 is true. System* (2) *experiences a PD bifurcation at E_2 if l_1,l_2 given in* (10) *and* (11) *are non-zero and h fluctuates in a close neighborhood of*

$$h_1=re^{1-\frac{1}{\sqrt{-1+b}}}-b(-2+\frac{e^{1-\frac{1}{\sqrt{-1+b}}}r}{\sqrt{-1+b}})-1.$$

Moreover, if $l_2>0$ (respectively $l_2<0$), then a period-2 orbit of the system (2) *emerges and it is stable (respectively, unstable).*

Next, we proceed to investigate the NS bifurcation at E_2 under condition (5) stated in Theorem 2.5. By applying a small perturbation δ ($|\delta| \lll 1$) to the bifurcation parameter around the critical value h_2, system (2) is changed to

$$\begin{cases} x_{n+1} = rx_n e^{1-x_n} - \frac{bx_n^2 y_n}{1+x_n^2} - (h+\delta)x_n, \\ y_{n+1} = \frac{bx_n^2 y_n}{1+x_n^2}. \end{cases} \tag{12}$$

We transform the fixed point E_2 to the origin by considering the change of variables $u_n = x_n - \frac{1}{\sqrt{b-1}}$, $v_n = y_n - \frac{-1-h+re^{1-\frac{1}{\sqrt{b-1}}}}{\sqrt{b-1}}$. After substituting $h = h_2$, system (12) is transformed into the following form:

$$\begin{bmatrix} u_{n+1} \\ v_{n+1} \end{bmatrix} = \begin{bmatrix} \frac{b+\frac{2e^{1-\frac{1}{\sqrt{-1+b}}}r}{\sqrt{-1+b}} - \frac{2be^{1-\frac{1}{\sqrt{-1+b}}}r}{\sqrt{-1+b}} - 2\delta + b\delta}{b} & -1 \\ \frac{2(\sqrt{-1+b}e^{1-\frac{1}{\sqrt{-1+b}}}r + \delta - b\delta)}{b} & 1 \end{bmatrix} \begin{bmatrix} u_n \\ v_n \end{bmatrix} + \begin{bmatrix} F(u_n, v_n) \\ G(u_n, v_n) \end{bmatrix}, \tag{13}$$

where

$$\begin{aligned}
F(u_n, v_n) &= a_1 u_n v_n + a_2 u_n^2 v_n + a_3 u_n^2 + a_4 u_n^3 + O((|u_n| + |v_n|)^4), \\
G(u_n, v_n) &= b_1 u_n v_n + b_2 u_n^2 v_n + b_3 u_n^2 + b_4 u_n^3 + O((|u_n| + |v_n|)^4), \\
a_1 &= -\frac{2(-1+b)^{3/2}}{b}, \\
a_2 &= -\frac{(-4+b)(-1+b)^2}{b^2}, \\
a_3 &= \frac{\left(\frac{(8-18b+(14+\sqrt{-1+b})b^2-4b^3)e^{1-\frac{1}{\sqrt{-1+b}}}r}{-1+b} + 2(-4+b)(-1+b)^{3/2}\delta\right)}{2b^2}, \\
a_4 &= \frac{\left(\frac{(-48+120b-96b^2+(23+3\sqrt{-1+b})b^3)e^{1-\frac{1}{\sqrt{-1+b}}}r}{\sqrt{-1+b}} - 24(-2+b)(-1+b)^2\delta\right)}{6b^3}, \\
b_1 &= \frac{2(-1+b)^{3/2}}{b}, \\
b_2 &= \frac{(-4+b)(-1+b)^2}{b^2}, \\
b_3 &= \frac{(-4+b)(-1+b)e^{-\frac{1}{\sqrt{-1+b}}}(er - \sqrt{-1+b}e^{\frac{1}{\sqrt{-1+b}}}\delta)}{b^2}, \\
b_4 &= \frac{4(-2+b)(-1+b)^{3/2}e^{-\frac{1}{\sqrt{-1+b}}}(-er + \sqrt{-1+b}e^{\frac{1}{\sqrt{-1+b}}}\delta)}{b^3}.
\end{aligned}$$

The characteristic equation of the Jacobian matrix of system (13) estimated at origin is

$$\xi^2 - \alpha(\delta)\xi + \beta(\delta) = 0, \tag{14}$$

where

$$\alpha(\delta) = 2 + \delta - \frac{2(\sqrt{-1+b}e^{1-\frac{1}{\sqrt{-1+b}}}r + \delta)}{b},$$
$$\beta(\delta) = 1 - \delta.$$

The complex solutions for (14) are calculated as:

$$\xi_{1,2} = \frac{\alpha(\delta)}{2} \pm \frac{i}{2}\sqrt{4\beta(\delta) - \alpha^2(\delta)}. \tag{15}$$

Moreover, we obtain

$$\left(\frac{d|\xi_1|}{d\delta}\right)_{\delta=0} = \left(\frac{d|\xi_2|}{d\delta}\right)_{\delta=0} = -\frac{1}{2} < 0.$$

Additionally, it is required that $\xi_{1,2}^i \neq 1$ when $\delta = 0$ for $i = 1, 2, 3, 4$, which corresponds to $\alpha(0) \neq -2, 2, 0, 1$. We obtain

$$\alpha(0) = 2 - \frac{2\sqrt{-1+b}e^{1-\frac{1}{\sqrt{-1+b}}}r}{b} < 2.$$

Moreover, $\alpha(0) \neq -2, 0, 1$ is equivalent to

$$r \neq \frac{2be^{-1+\frac{1}{\sqrt{b-1}}}}{\sqrt{b-1}}, \frac{be^{-1+\frac{1}{\sqrt{b-1}}}}{\sqrt{b-1}}, \frac{be^{-1+\frac{1}{\sqrt{b-1}}}}{2\sqrt{b-1}}. \tag{16}$$

Next, to change (13) into normal form at $\delta = 0$, we use the following similarity transformation:

$$\begin{bmatrix} u_n \\ v_n \end{bmatrix} = \begin{bmatrix} -1 & 0 \\ \frac{\sqrt{-1+b}e^{1-\frac{1}{\sqrt{-1+b}}}r}{b} & -\frac{1}{2}\sqrt{4-(2-\frac{2\sqrt{-1+b}e^{1-\frac{1}{\sqrt{-1+b}}}r}{b})^2} \end{bmatrix} \begin{bmatrix} X_n \\ Y_n \end{bmatrix}. \tag{17}$$

Upon application of the mapping (17), system (13) takes the following form:

(18)

$$\begin{bmatrix} X_{n+1} \\ Y_{n+1} \end{bmatrix} = \begin{bmatrix} 1-\frac{\sqrt{-1+b}e^{1-\frac{1}{\sqrt{-1+b}}}r}{b} & -\frac{1}{2}\sqrt{4-(2-\frac{2\sqrt{-1+b}e^{1-\frac{1}{\sqrt{-1+b}}}r}{b})^2} \\ 1-\frac{\sqrt{-1+b}e^{1-\frac{1}{\sqrt{-1+b}}}r}{b} & \frac{1}{2}\sqrt{4-(2-\frac{2\sqrt{-1+b}e^{1-\frac{1}{\sqrt{-1+b}}}r}{b})^2} \end{bmatrix} \begin{bmatrix} X_n \\ Y_n \end{bmatrix} + \begin{bmatrix} \Gamma(X_n,Y_n) \\ \Upsilon(X_n,Y_n) \end{bmatrix},$$

where

$$\Gamma(X_n,Y_n) = c_1X_n^2 + c_2X_n^3 + c_3X_nY_n + c_4X_n^2Y_n + O((|X_n|+|Y_n|)^4),$$
$$\Upsilon(X_n,Y_n) = d_1X_nY_n + d_2X_n^2Y_n + d_3X_n^2 + d_4X_n^3 + O((|X_n|+|Y_n|)^4),$$

where the values of coefficients are given in Appendix B. Then map (18) can undergo NS bifurcation if the following quantity is non-zero:

$$L = \left(-Re\left(\frac{(1-2\xi_1)\xi_2^2}{1-\xi_1}\tau_{20}\tau_{11}\right) - \frac{1}{2}|\tau_{11}|^2 - |\tau_{02}|^2 + Re(\xi_2\tau_{21})\right)_{\delta=0}, \tag{19}$$

where

$$\tau_{20} = \frac{1}{8}\left(\Gamma_{X_nX_n} - \Gamma_{Y_nY_n} + 2\Upsilon_{X_nY_n} + i(\Upsilon_{X_nX_n} - \Upsilon_{Y_nY_n} - 2\Gamma_{X_nY_n})\right),$$
$$\tau_{11} = \frac{1}{4}\left(\Gamma_{X_nX_n} + \Gamma_{Y_nY_n} + i(\Upsilon_{X_nX_n} + \Upsilon_{Y_nY_n})\right),$$
$$\tau_{02} = \frac{1}{8}\left(\Gamma_{X_nX_n} - \Gamma_{Y_nY_n} - 2\Upsilon_{X_nY_n} + i(\Upsilon_{X_nX_n} - \Upsilon_{Y_nY_n} + 2\Gamma_{X_nY_n})\right),$$
$$\tau_{21} = \frac{1}{16}\left(\Gamma_{X_nX_nX_n} + \Gamma_{X_nY_nY_n} + \Upsilon_{X_nX_nY_n} + \Upsilon_{Y_nY_nY_n} + i(\Upsilon_{X_nX_nX_n} + \Upsilon_{X_nY_nY_n} - \Gamma_{X_nX_nY_n} - \Gamma_{Y_nY_nY_n})\right).$$

Therefore, the result derived from the above analysis is as follows:

Theorem 3.2. *Suppose that condition (5) of Theorem 2.5 holds true. If the condition* (16) *is satisfied and L given in* (19) *holds a non-zero value, then system* (2) *experiences NS bifurcation at E_2 as long as h fluctuates in a close neighbourhood of* $h_2 = \frac{r(-1+\sqrt{-1+b})e^{1-\frac{1}{\sqrt{-1+b}}}}{\sqrt{-1+b}} - 1$. *Furthermore, in instances where L is negative (alternatively, positive), the NS bifurcation encountered in system* (2) *at E_2 is categorized as supercritical (subcritical), giving rise to the presence of a unique closed invariant curve originating from E_2 that is attracting (repelling).*

4. Chaos Control

The aim of optimizing dynamical systems in order to meet particular performance criteria and minimize chaotic behavior is a highly desirable objective. Chaos control techniques are extensively employed in several fields of applied research and engineering. Historically, bifurcations and unstable oscillations have been regarded in a negative light within the field of mathematical biology due to their detrimental impact on the reproductive capacity of biological populations. It is possible to design a controller that may modify the bifurcation features of a nonlinear system in order to achieve specific desired dynamical attributes and effectively control chaos under the effects of PD and NS bifurcations. Multiple strategies exist for the purpose of managing chaos in a discrete-time system. This section is dedicated to examining two distinct control methods, namely state feedback control and hybrid control approaches.

Initially, the state feedback control strategy, as described in references [62, 63], is employed to regulate the chaotic behavior of the system (2). The suggested methodology entails the conversion of the chaotic system into a piecewise linear system in order to obtain an optimal controller that effectively reduces the upper limit. Following this, the problem of optimization is carried out subject to certain constraints. The technique described above is utilized in order to attain stabilization of chaotic orbits situated at an unstable fixed point within the system (2). The controlled system under consideration for this purpose is as follows:

$$\begin{cases} x_{n+1} = rx_n e^{1-x_n} - \frac{bx_n^2 y_n}{1+x_n^2} - hx_n - U_n, \\ y_{n+1} = \frac{bx_n^2 y_n}{1+x_n^2}, \end{cases} \tag{20}$$

where $U_n = \kappa_1\left(x_n - \frac{1}{\sqrt{b-1}}\right) + \kappa_2\left(y_n - \frac{-1-h+re^{1-\frac{1}{\sqrt{b-1}}}}{\sqrt{b-1}}\right)$ is the feedback controlling force with feedback gains κ_1 and κ_2. Through simple calculations, it is obtained that for system (20) we have

$$J(E_2) = \begin{bmatrix} \frac{-2(1+h)+b(2+h-\kappa_1)-\frac{(-2\sqrt{-1+b}+b+\sqrt{-1+b}b)e^{1-\frac{1}{\sqrt{-1+b}}}r}{\sqrt{-1+b}}}{b} & -1-\kappa_2 \\ -\frac{2(-1+b)e^{-\frac{1}{\sqrt{-1+b}}}(e^{\frac{1}{\sqrt{-1+b}}}(1+h)-er)}{b} & 1 \end{bmatrix}. \tag{21}$$

The matrix $J(E_2)$ has the following characteristic equation:

$$\xi^2+K_1\xi+K_0=0, \tag{22}$$

where

$$K_1=\frac{2+2h-2e^{1-\frac{1}{\sqrt{-1+b}}}r+b(-3-h+\kappa_1+e^{1-\frac{1}{\sqrt{-1+b}}}r+\frac{e^{1-\frac{1}{\sqrt{-1+b}}}r}{\sqrt{-1+b}})}{b},$$

$$K_0=-h-\kappa_1-2\kappa_2-2h\kappa_2+\frac{2(1+h)\kappa_2}{b}-\frac{2e^{1-\frac{1}{\sqrt{-1+b}}}\kappa_2 r}{b}$$
$$+\frac{e^{1-\frac{1}{\sqrt{-1+b}}}(-1+\sqrt{-1+b}+2\sqrt{-1+b}\kappa_2)r}{\sqrt{-1+b}}.$$

Let ξ_1 and ξ_2 be the roots of (22), then we have

$$\xi_1+\xi_2=-\frac{2+2h-2e^{1-\frac{1}{\sqrt{-1+b}}}r+b(-3-h+\kappa_1+e^{1-\frac{1}{\sqrt{-1+b}}}r+\frac{e^{1-\frac{1}{\sqrt{-1+b}}}r}{\sqrt{-1+b}})}{b}, \tag{23}$$

$$\xi_1\xi_2=-h-\kappa_1-2\kappa_2-2h\kappa_2+\frac{2(1+h)\kappa_2}{b}-\frac{2e^{1-\frac{1}{\sqrt{-1+b}}}\kappa_2 r}{b} \tag{24}$$

$$+\frac{e^{1-\frac{1}{\sqrt{-1+b}}}(-1+\sqrt{-1+b}+2\sqrt{-1+b}\kappa_2)r}{\sqrt{-1+b}}. \tag{25}$$

Then, the lines of marginal stability are derived by solving $\xi_1=\pm1$ and $\xi_1\xi_2=1$. These conditions ensure that $|\xi_{1,2}|<1$. Assume that $\xi_1\xi_2=1$, then equation (25) implies that

(26)
$$L_1:-\kappa_1-\left(\frac{2(-1+b)e^{-\frac{1}{\sqrt{-1+b}}}(e^{\frac{1}{\sqrt{-1+b}}}(1+h)-er)}{b}\right)\kappa_2-1-h+e^{1-\frac{1}{\sqrt{-1+b}}}(r-\frac{r}{\sqrt{-1+b}})=0.$$

Next, we take $\xi_1=1$ and utilizing equations (23) and (25), we obtain

$$L_2:\kappa_2=-1. \tag{27}$$

Next, we take $\xi_1=-1$ and utilizing equations (23) and (25), we obtain

$$L_3:-2\kappa_1+\left(-\frac{2(-1+b)e^{-\frac{1}{\sqrt{-1+b}}}(e^{\frac{1}{\sqrt{-1+b}}}(1+h)-er)}{b}\right)\kappa_2+L_{30}=0, \tag{28}$$

where

$$L_{30}=-\frac{2(1+h-e^{1-\frac{1}{\sqrt{-1+b}}}r+b(-2+\frac{e^{1-\frac{1}{\sqrt{-1+b}}}r}{\sqrt{-1+b}}))}{b}.$$

The stable eigenvalues are enclosed within the triangular region bounded L_1, L_2, and L_3.

Next, we apply the hybrid control approach [64] for controlling chaos through both types of bifurcation effects. The hybrid control technique refers to a methodology that integrates the utilization of state feedback and parameter adjustment in order to achieve stabilization of unstable periodic orbits that are present within the chaotic attractor of a given system. The controlled system of (2), when hybrid control approach is used, becomes

$$\begin{cases} x_{n+1} = \rho\left(rx_n e^{1-x_n} - \frac{bx_n^2 y_n}{1+x_n^2} - hx_n\right) + (1-\rho)x_n, \\ y_{n+1} = \frac{\rho b x_n^2 y_n}{1+x_n^2} + (1-\rho)y_n, \end{cases} \tag{29}$$

where $\rho \in (0,1)$ is the control parameter. The same fixed points are shared by system (29) and system (2). We obtain

$$J(E_2) = \begin{bmatrix} 1 + \frac{((-2+b)(1+h) - \frac{(-2\sqrt{-1+b}+b+\sqrt{-1+b}b)e^{1-\frac{1}{\sqrt{-1+b}}}r}{\sqrt{-1+b}})\rho}{b} & -\rho \\ -\frac{2(-1+b)e^{-\frac{1}{\sqrt{-1+b}}}(e^{\frac{1}{\sqrt{-1+b}}}(1+h)-er)\rho}{b} & 1 \end{bmatrix}, \tag{30}$$

then, its characteristic equation is as follows:

$$\xi^2 + K_1\xi + K_0 = 0, \tag{31}$$

where

$$K_1 = -2 + \frac{(-(-2+b)(1+h) + \frac{(-2\sqrt{-1+b}+b+\sqrt{-1+b}b)e^{1-\frac{1}{\sqrt{-1+b}}}r}{\sqrt{-1+b}})\rho}{b},$$

$$K_0 = \frac{1}{\sqrt{-1+b}b} e^{-\frac{1}{\sqrt{-1+b}}}\Bigg(2\sqrt{-1+b}(e^{\frac{1}{\sqrt{-1+b}}}(1+h) - er)(-1+\rho)\rho$$
$$+ b(er\rho(-1-\sqrt{-1+b}+2\sqrt{-1+b}\rho) + \sqrt{-1+b}e^{\frac{1}{\sqrt{-1+b}}}(1+(1+h)\rho - 2(1+h)\rho^2))\Bigg).$$

Theorem 4.1. *The fixed point E_2 of the controlled system* (29) *is LAS if*

$$|K_1| < 1 + K_0 < 2.$$

5. NUMERICAL EXAMPLES

In this section, we substantiate our theoretical findings for system (2) by the use of numerical simulations. The numerical simulations will involve the representation of bifurcation diagrams, phase portraits, time series plots, and graphs depicting the maximum Lyapunov exponent (MLE).

We assume that $r = 2.7, b = 4.5$. Then, system (2) experiences both PD bifurcation and NS bifurcation as h varies in small neighborhoods of $h_1 \approx 1.956299$ and $h_2 \approx 1.00178$, respectively. The positive fixed point is obtained as $E_2 = (0.534522, 0.718501)$ for $h = h_1$. The eigenvalues of $J(E_2)$ are $\xi_1 = -1$ and $\xi_2 = -0.045483$ with $|\xi_2| \neq 1$. The bifurcation diagrams of system (2) are given in Figures 1a and 1b, while the MLE is plotted in Figure 1c by using initial conditions $x_0 = 0.55$ and $y_0 = 0.75$ and varying $h \in [1.90, 2.80]$.

Moreover, the positive fixed point is obtained as $E_2 = (0.534522, 1.22871)$ for $h = h_2$. The eigenvalues of $J(E_2)$ are $\xi_{1,2} = -0.787885 \pm 0.615822i$ with $|\xi_{1,2}| = 1$. Moreover, some careful calculations give

$$\tau_{20} = 0.153152 + 0.293762i, \tau_{11} = -0.84014 + 1.4836i,$$

$$\tau_{02} = -0.993291 + 1.18984i, \tau_{21} = 2.001 + 3.68923i.$$

Thus, it is obtained that $L = -2.88929 < 0$, which proves the correctness of Theorem 3.2. The bifurcation diagrams of system (2) are given in Figures 2a and 2b, while the MLE is plotted in Figure 2c by using initial conditions $x_0 = 0.55$ and $y_0 = 1.25$ and varying $h \in [0.91, 1.11]$.

(A) Bifurcation diagram in (h, x_n) plane

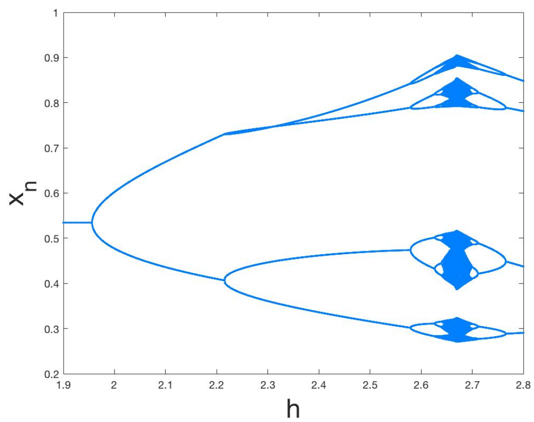

(B) Bifurcation diagram in (h, y_n) plane

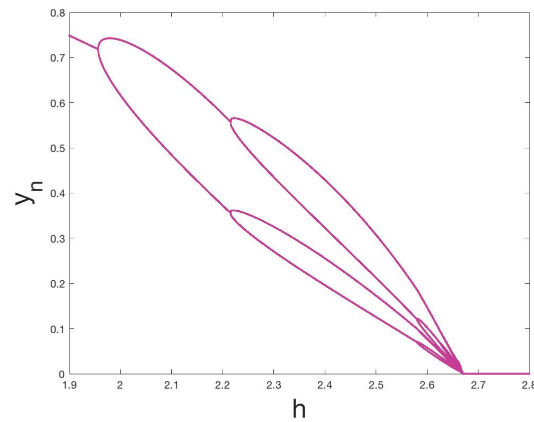

(C) MLE graph

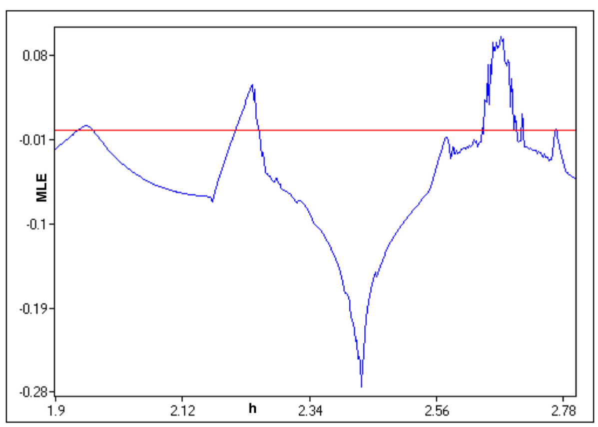

FIGURE 1. Bifurcation diagrams and MLE graph of system (2) by fixing $r = 2.7, b = 4.5, x_0 = 0.55, y_0 = 0.75$, and varying h in $[1.90, 2.80]$.

(A) Bifurcation diagram in (h, x_n) plane

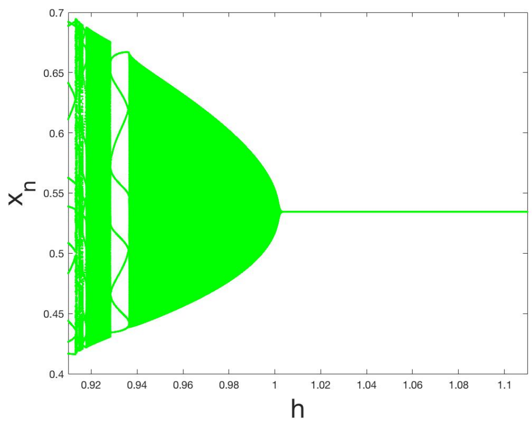

(B) Bifurcation diagram in (h, y_n) plane

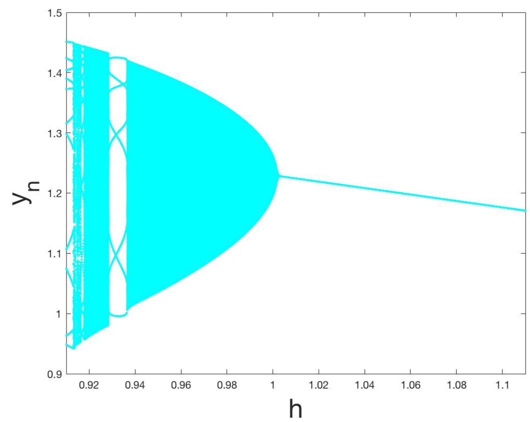

(C) MLE graph

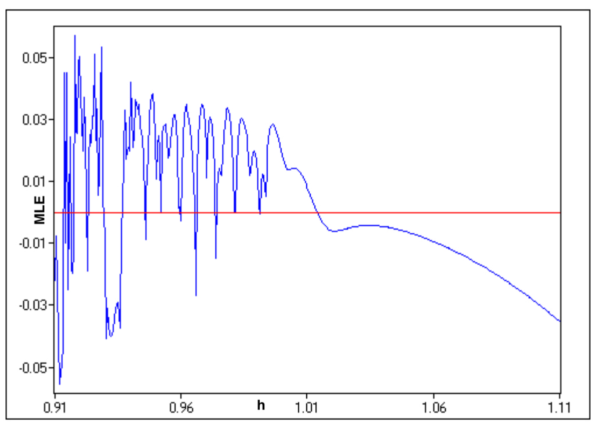

FIGURE 2. Bifurcation diagrams of system (2) with respect to h for $h \in [0.91, 1.11]$. Fixed parameter values are $r = 2.7, b = 4.5$ and initial conditions are $x_0 = 0.55, y_0 = 1.25$.

Next, Figures 3a-3i show phase portraits of system (2) for various values of h. One can observe that E_2 is LAS for $1.00178 < h < 1.956299$ but loses stability at $h = 1.00178$, when the system (2) experiences NS bifurcation. For $h \leq 1.00178$, an invariant curve emerges from E_2, the radius of which grows as h grows. Moreover, when $h = 1.956299$, the system (2) goes through PD bifurcation.

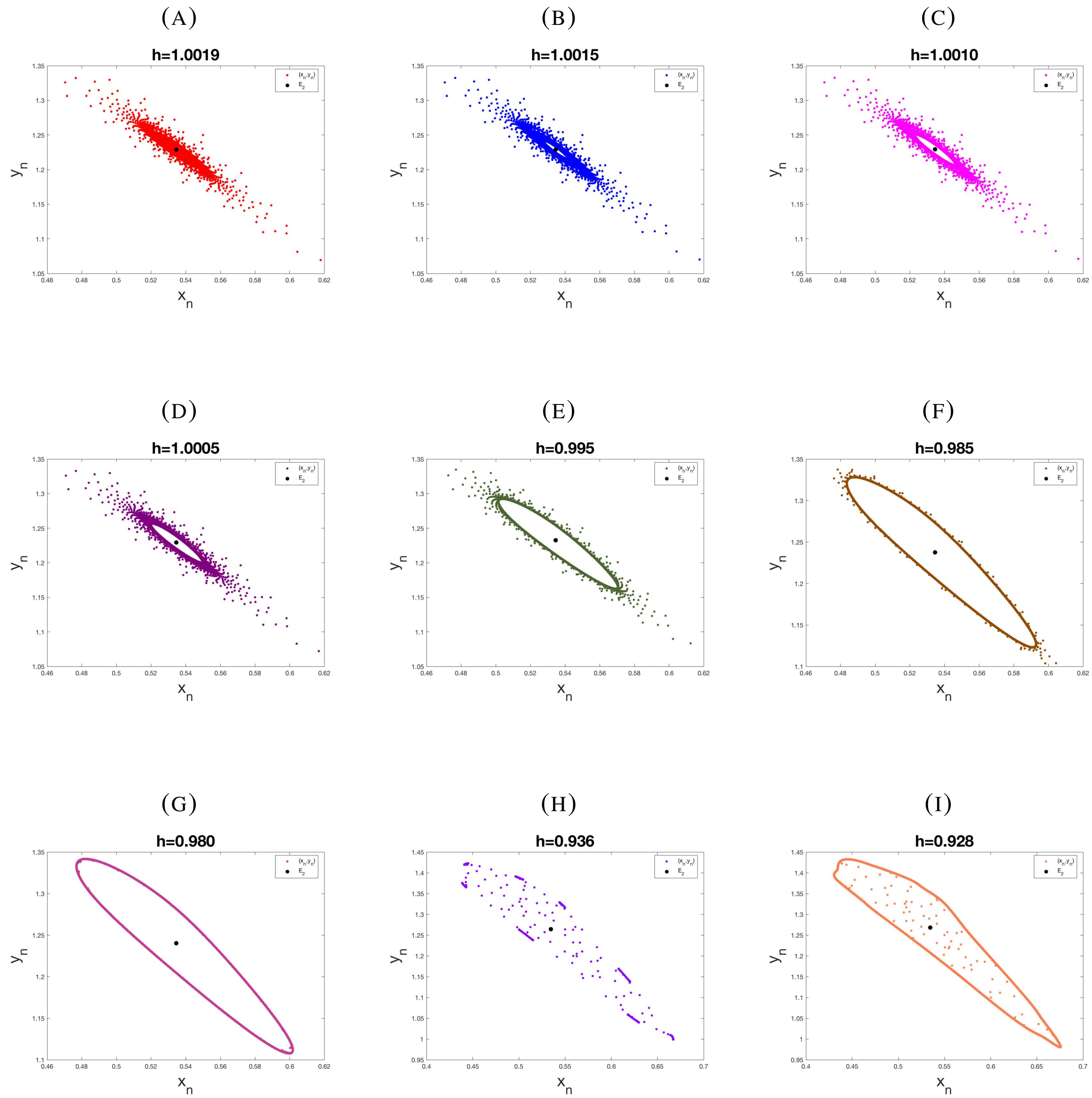

FIGURE 3. Phase portraits of (2) for various values of h and fixing $r = 2.7, b = 4.5, x_0 = 0.55, y_0 = 1.25$.

The harvesting rate affecting the prey population, plays a crucial role in the stability of the ecosystem. The existence of two critical values, h_1 and h_2, suggests that there exists an optimal level of harvesting in the system (2). When h is too low, it can lead to overpopulation of prey species, which may outcompete resources and negatively impact both the predator and prey populations. Conversely, excessive harvesting when h is too high can decimate the prey population, leading to food scarcity and a decline in the predator population.

The efficacy of the hybrid control approach will next be evaluated. We assume $\rho = 0.985, r = 2.7, b = 4.5$ and vary h for the controlled system (29). If $0.946864 < h < 2.026469$, the positive fixed point E_2 is LAS. One can observe that the stability region has been expanded. The bifurcation diagrams are presented in Figures 4a and 4b by using initial conditions $x_0 = 0.55, y_0 = 1.25$ and varying $h \in [0.91, 1.11]$. Moreover, bifurcation diagrams are presented in Figures 4c and 4d by using initial conditions $x_0 = 0.55, y_0 = 0.75$ and varying $h \in [1.90, 2.80]$.

Next, we aim to evaluate the efficacy of the feedback control technique. Considering $r = 2.7, b = 4.5, h = 0.98$, as well as the initial conditions $x_0 = 0.55$ and $y_0 = 1.25$ for the controlled system (20), the marginal stability lines are as follows:

$$L_1 : \kappa_2 = -0.006034 + 0.277035\kappa_1,$$

$$L_2 : \kappa_2 = -1,$$

and

$$L_1 : \kappa_2 = -0.120208 + 0.55407\kappa_1.$$

Figure 5a depicts the stability region bounded by lines L_1, L_2, and L_3 for system (20). The fixed point E_2 of system (2) is shown to be unstable for the given parametric values. The controlled system (20) is examined with feedback gains $\kappa_1 = -3.20$ and $\kappa_2 = -0.91$. Figure 5 illustrates the graph of x_n as shown in Figure 5c, y_n as shown in Figure 5d, and the phase portrait as presented in Figure 5b for the system (20). Therefore, it may be deduced that the use of the feedback control methodology seems to be effective in controlling bifurcation and chaos.

(A) Bifurcation diagram in (h, x_n) plane of system (29)

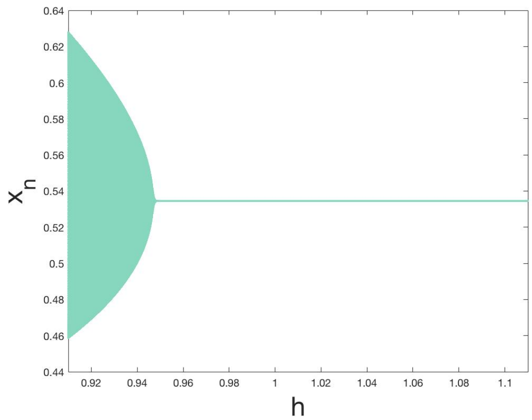

(B) Bifurcation diagram in (h, y_n) plane of system (29)

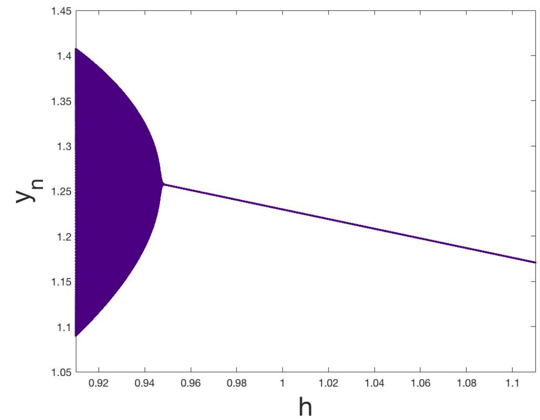

(C) Bifurcation diagram in (h, x_n) plane of system (29)

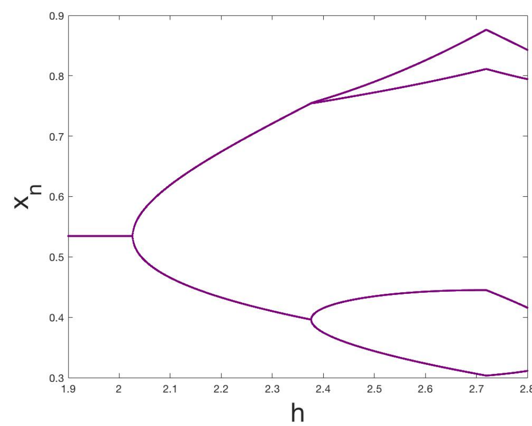

(D) Bifurcation diagram in (h, y_n) plane of system (29)

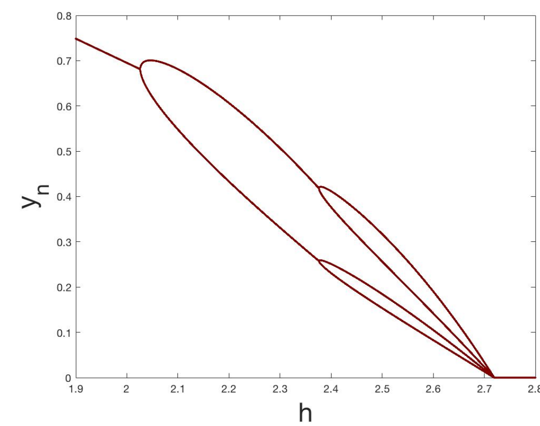

FIGURE 4. Bifurcation diagrams of system (29) by fixing $\rho = 0.985, r = 2.7, b = 4.5$ (4a, 4b) $x_0 = 0.55, y_0 = 1.25$ and varying $h \in [0.91, 1.11]$, (4c, 4d) $x_0 = 0.55, y_0 = 0.75$ and varying $h \in [1.90, 2.80]$

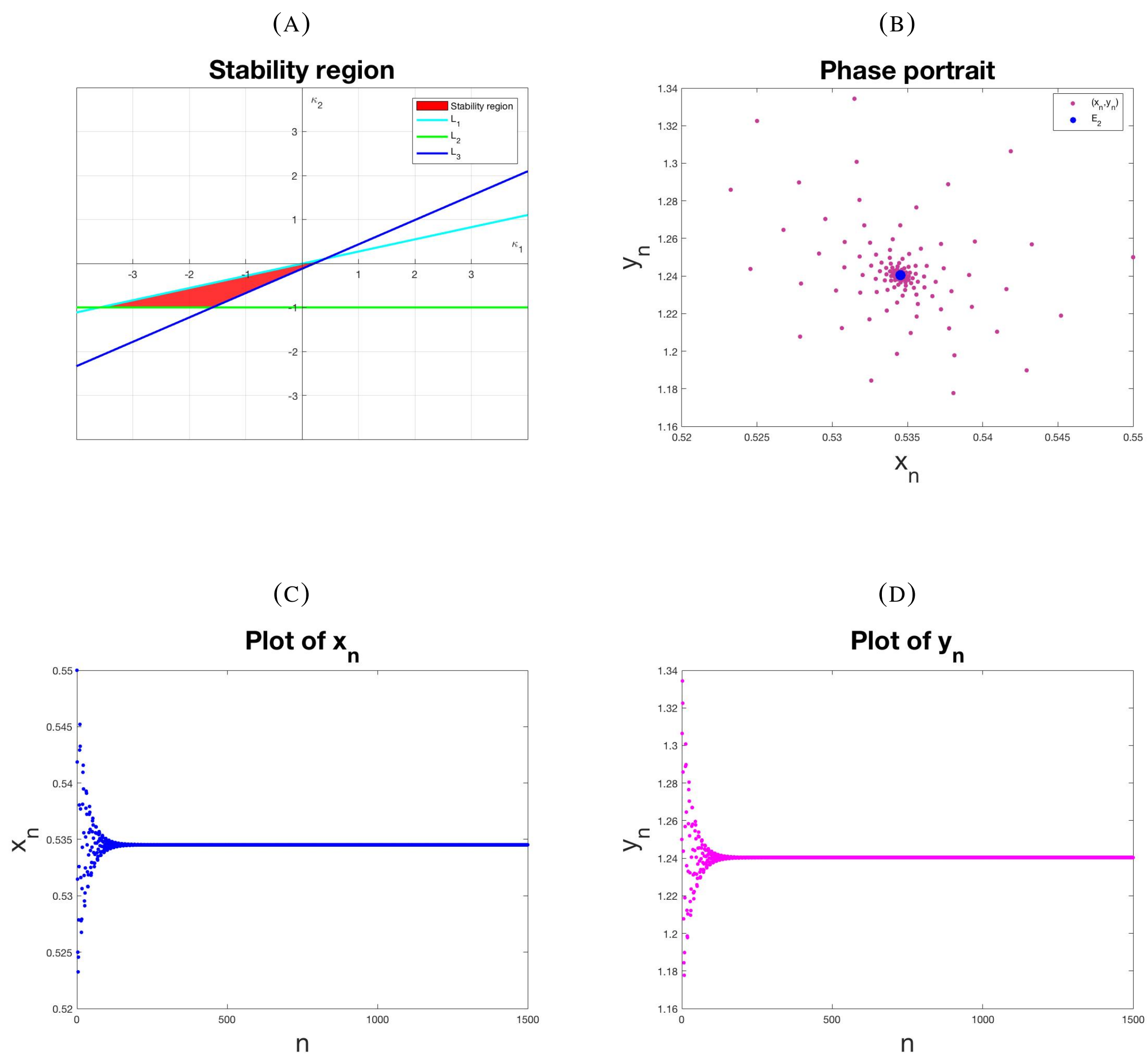

FIGURE 5. Stability region, phase portrait, and time series plots of system (20) using $r = 2.7, b = 4.5, h = 0.98$ and initial conditions are $x_0 = 0.55, y_0 = 1.25$.

6. CONCLUSION

In an ecosystem, the harvesting effect is critical in determining the stability of predator-prey relationships. We present and investigate the complex dynamics of a discrete-time predator-prey system with a harvesting effect in the present study. Fixed points' presence and stability are studied. Furthermore, a thorough examination of local bifurcations at the positive fixed point is carried out. The study shows that system (2) undergoes both PD and NS bifurcation. To control bifurcation and chaos, feedback control and hybrid control systems are used. As a result, effective control over a wide variety of parameters is achieved for both forms of bifurcation. Furthermore, numerical simulations are run to validate the previously stated theoretical results. Several visual representations are used in these simulations, including bifurcation diagrams, MLE graphs, phase portraits, and time series plots. It is discovered that the positive fixed point is stable when the harvesting parameter h is within the optimal range $h_1 < h < h_2$. Our findings highlight the necessity of maintaining a moderate amount of harvesting, as it appears to benefit both predator and prey populations, promoting ecosystem stability and sustainability. The outcome of this study has important implications for conservation and resource management techniques, highlighting the importance of carefully considering harvesting rates in ecological systems.

APPENDIX A

$$c_1 = \frac{4(-1+b)^{5/2}e^{\frac{1}{\sqrt{-1+b}}} - (3+(-4+\sqrt{-1+b})b+b^2)er}{(-1+b)b(2be^{\frac{1}{\sqrt{-1+b}}} - \sqrt{-1+b}er)},$$

$$c_2 = e^{-\frac{1}{\sqrt{-1+b}}}\left(-2(-1+b)e^{\frac{1}{\sqrt{-1+b}}} + \sqrt{-1+b}er\right)\left(6(-1+b)^{5/2}(-4+3b)e^{\frac{1}{\sqrt{-1+b}}} + (24-60b+(49 - 3\sqrt{-1+b})b^2 - 12b^3)er\right)\Big/\left(24\sqrt{-1+b}b^2(-2be^{\frac{1}{\sqrt{-1+b}}} + \sqrt{-1+b}er)\right),$$

$$c_3 = e^{-\frac{1}{\sqrt{-1+b}}}\left(2(-1+b)e^{\frac{1}{\sqrt{-1+b}}} - \sqrt{-1+b}er\right)\left(2(-2+b)(-1+b)^{5/2}e^{\frac{1}{\sqrt{-1+b}}} + (4+(-7+\sqrt{-1+b})b + 4b^2 - b^3)er\right)\Big/\left(4(-1+b)b(2be^{\frac{1}{\sqrt{-1+b}}} - \sqrt{-1+b}er)\right),$$

$$c_4 = \frac{e^{\frac{1}{\sqrt{-1+b}}}(-2(-1+b)^{5/2}(2+b)e^{\frac{1}{\sqrt{-1+b}}} + (2+(-1+\sqrt{-1+b})b - 2b^2 + b^3)er)}{(-1+b)b(2(-1+b)e^{\frac{1}{\sqrt{-1+b}}} - \sqrt{-1+b}er)(2be^{\frac{1}{\sqrt{-1+b}}} - \sqrt{-1+b}er)},$$

$$c_5 = \frac{e^{\frac{2}{\sqrt{-1+b}}}(6(-1+b)^{5/2}(-4-b+b^2)e^{\frac{1}{\sqrt{-1+b}}} + (12-21b+(4-3\sqrt{-1+b})b^2+9b^3-3b^4)er)}{3\sqrt{-1+b}b^2(-2(-1+b)e^{\frac{1}{\sqrt{-1+b}}} + \sqrt{-1+b}er)^2(-2be^{\frac{1}{\sqrt{-1+b}}} + \sqrt{-1+b}er)},$$

$$c_6 = \frac{e^{\frac{1}{\sqrt{-1+b}}}(2(-1+b)^{5/2}(-12+b+2b^2)e^{\frac{1}{\sqrt{-1+b}}} + (16-34b+(19-3\sqrt{-1+b})b^2+2b^3-2b^4)er)}{2\sqrt{-1+b}b^2(-2(-1+b)e^{\frac{1}{\sqrt{-1+b}}} + \sqrt{-1+b}er)(-2be^{\frac{1}{\sqrt{-1+b}}} + \sqrt{-1+b}er)},$$

$$c_7 = \frac{2(-1+b)^{5/2}(-12+5b+b^2)e^{\frac{1}{\sqrt{-1+b}}} - (-20+47b+(-34+3\sqrt{-1+b})b^2+5b^3+b^4)er}{4\sqrt{-1+b}b^2(-2be^{\frac{1}{\sqrt{-1+b}}} + \sqrt{-1+b}er)},$$

$$c_8 = \frac{2(-1+b)e^{\frac{1}{\sqrt{-1+b}}} - \sqrt{-1+b}er}{b(2be^{\frac{1}{\sqrt{-1+b}}} - \sqrt{-1+b}er)},$$

$$c_9 = \frac{(-4+b)(-1+b)^{3/2}e^{\frac{1}{\sqrt{-1+b}}}}{b^2(-2be^{\frac{1}{\sqrt{-1+b}}} + \sqrt{-1+b}er)},$$

$$c_{10} = \frac{(-4+b)(-1+b)^{3/2}e^{\frac{2}{\sqrt{-1+b}}}}{b^2(-2(-1+b)e^{\frac{1}{\sqrt{-1+b}}} + \sqrt{-1+b}er)(-2be^{\frac{1}{\sqrt{-1+b}}} + \sqrt{-1+b}er)},$$

$$c_{11} = \frac{(-4+b)(-1+b)^{3/2}(-2(-1+b)e^{\frac{1}{\sqrt{-1+b}}} + \sqrt{-1+b}er)}{4b^2(-2be^{\frac{1}{\sqrt{-1+b}}} + \sqrt{-1+b}er)},$$

$$c_{12} = -\frac{2e^{\frac{1}{\sqrt{-1+b}}}}{2b^2e^{\frac{1}{\sqrt{-1+b}}} - \sqrt{-1+b}ber},$$

$$d_1 = \Big(-8\sqrt{-1+b}(1-3b+2b^2)e^{\frac{2}{\sqrt{-1+b}}} + 2(7+(-15+\sqrt{-1+b})b+8b^2)e^{1+\frac{1}{\sqrt{-1+b}}}r - (-6\sqrt{-1+b}$$
$$+b+4\sqrt{-1+b}b)e^2r^2\Big)\Big/\Big(b(2(-1+b)e^{\frac{1}{\sqrt{-1+b}}} - \sqrt{-1+b}er)(2be^{\frac{1}{\sqrt{-1+b}}} - \sqrt{-1+b}er)\Big),$$

$$d_2 = e^{-\frac{1}{\sqrt{-1+b}}}\Big(-4\sqrt{-1+b}(-2+7b-7b^2+2b^3)e^{\frac{2}{\sqrt{-1+b}}} + 2(-8-(-21+\sqrt{-1+b})b-17b^2$$
$$+4b^3)e^{1+\frac{1}{\sqrt{-1+b}}}r + (-8\sqrt{-1+b}+b+8\sqrt{-1+b}b-2\sqrt{-1+b}b^2)e^2r^2\Big)\Big/\Big(4b(2be^{\frac{1}{\sqrt{-1+b}}} - \sqrt{-1+b}er)\Big),$$

$$d_3 = e^{\frac{1}{\sqrt{-1+b}}}\Big(4\sqrt{-1+b}(2-5b+b^2+2b^3)e^{\frac{2}{\sqrt{-1+b}}} - 2(6+(-9+\sqrt{-1+b})b-b^2+4b^3)e^{1+\frac{1}{\sqrt{-1+b}}}r$$
$$+(-4\sqrt{-1+b}+b+2\sqrt{-1+b}b^2)e^2r^2\Big)\Big/\Big(b(2be^{\frac{1}{\sqrt{-1+b}}} - \sqrt{-1+b}er)(-2(-1+b)e^{\frac{1}{\sqrt{-1+b}}} + \sqrt{-1+b}er)^2\Big),$$

$$d_4 = e^{-\frac{1}{\sqrt{-1+b}}}\Big(12(-1+b)^{5/2}(4-11b+6b^2)e^{\frac{2}{\sqrt{-1+b}}} - 2(-1+b)(-48+150b+(-145+3\sqrt{-1+b})b^2$$
$$+42b^3)e^{1+\frac{1}{\sqrt{-1+b}}}r + (-48\sqrt{-1+b}+120\sqrt{-1+b}b-(3+97\sqrt{-1+b})b^2$$
$$+3(1+8\sqrt{-1+b})b^3)e^2r^2\Big)\Big/\Big(24\sqrt{-1+b}b^2(-2be^{\frac{1}{\sqrt{-1+b}}} + \sqrt{-1+b}er)\Big),$$

$$d_5 = \Big(4(-1+b)^{5/2}(12-29b+9b^2+2b^3)e^{\frac{2}{\sqrt{-1+b}}} - 2(-1+b)(-44+125b+(-103+3\sqrt{-1+b})b^2+17b^3$$
$$+4b^4)e^{1+\frac{1}{\sqrt{-1+b}}}r + (-40\sqrt{-1+b}+94\sqrt{-1+b}b-(3+67\sqrt{-1+b})b^2+(3+10\sqrt{-1+b})b^3$$
$$+2\sqrt{-1+b}b^4)e^2r^2\Big)\Big/\Big(4\sqrt{-1+b}b^2(-2(-1+b)e^{\frac{1}{\sqrt{-1+b}}} + \sqrt{-1+b}er)(-2be^{\frac{1}{\sqrt{-1+b}}} + \sqrt{-1+b}er)\Big),$$

$$d_6 = e^{\frac{1}{\sqrt{-1+b}}}\bigg(4(-1+b)^{5/2}(12-25b+4b^3)e^{\frac{2}{\sqrt{-1+b}}} - 2(-1+b)(-40+100b+(-61+3\sqrt{-1+b})b^2-8b^3 + 8b^4)e^{1+\frac{1}{\sqrt{-1+b}}}r + (-32\sqrt{-1+b}+68\sqrt{-1+b}b-(3+37\sqrt{-1+b})b^2+(3-4\sqrt{-1+b})b^3 + 4\sqrt{-1+b}b^4)e^2r^2\bigg)\bigg/\bigg(2\sqrt{-1+b}b^2(-2(-1+b)e^{\frac{1}{\sqrt{-1+b}}}+\sqrt{-1+b}er)^2(-2be^{\frac{1}{\sqrt{-1+b}}}+\sqrt{-1+b}er)\bigg),$$

$$d_7 = e^{\frac{2}{\sqrt{-1+b}}}\bigg(12(-1+b)^{5/2}(4-7b-3b^2+2b^3)e^{\frac{2}{\sqrt{-1+b}}} - 2(-1+b)(-36+75b+(-19+3\sqrt{-1+b})b^2 - 33b^3+12b^4)e^{1+\frac{1}{\sqrt{-1+b}}}r + (-24\sqrt{-1+b}+42\sqrt{-1+b}b-(3+7\sqrt{-1+b})b^2+(3-18\sqrt{-1+b})b^3 + 6\sqrt{-1+b}b^4)e^2r^2\bigg)\bigg/\bigg(3\sqrt{-1+b}b^2(-2(-1+b)e^{\frac{1}{\sqrt{-1+b}}}+\sqrt{-1+b}er)^3(-2be^{\frac{1}{\sqrt{-1+b}}}+\sqrt{-1+b}er)\bigg),$$

$$d_8 = -\frac{(-4+b)(-1+b)^{3/2}((1-2b)e^{\frac{1}{\sqrt{-1+b}}}+\sqrt{-1+b}er)}{2b^2(-2be^{\frac{1}{\sqrt{-1+b}}}+\sqrt{-1+b}er)},$$

$$d_9 = -\frac{2(-4+b)(-1+b)^{3/2}e^{\frac{2}{\sqrt{-1+b}}}((1-2b)e^{\frac{1}{\sqrt{-1+b}}}+\sqrt{-1+b}er)}{b^2(-2(-1+b)e^{\frac{1}{\sqrt{-1+b}}}+\sqrt{-1+b}er)^2(-2be^{\frac{1}{\sqrt{-1+b}}}+\sqrt{-1+b}er)},$$

$$d_{10} = -\frac{2(-4+b)(-1+b)^{3/2}e^{\frac{1}{\sqrt{-1+b}}}((1-2b)e^{\frac{1}{\sqrt{-1+b}}}+\sqrt{-1+b}er)}{b^2(-2(-1+b)e^{\frac{1}{\sqrt{-1+b}}}+\sqrt{-1+b}er)(-2be^{\frac{1}{\sqrt{-1+b}}}+\sqrt{-1+b}er)},$$

$$d_{11} = \frac{2(-1+b)^2e^{\frac{1}{\sqrt{-1+b}}}-(-2+b)\sqrt{-1+b}er}{b(2be^{\frac{1}{\sqrt{-1+b}}}-\sqrt{-1+b}er)},$$

$$d_{12} = -\frac{2e^{\frac{1}{\sqrt{-1+b}}}(2(-1+b)^2e^{\frac{1}{\sqrt{-1+b}}}-(-2+b)\sqrt{-1+b}er)}{b(2(-1+b)e^{\frac{1}{\sqrt{-1+b}}}-\sqrt{-1+b}er)(2be^{\frac{1}{\sqrt{-1+b}}}-\sqrt{-1+b}er)}.$$

APPENDIX B

$$c_1 = -\frac{(4-6b+(2+\sqrt{-1+b})b^2)e^{1-\frac{1}{\sqrt{-1+b}}}r}{2(-1+b)b^2},$$

$$c_2 = \frac{(-24+42b-6b^2+(-19+3\sqrt{-1+b})b^3+6b^4)e^{1-\frac{1}{\sqrt{-1+b}}}r}{6\sqrt{-1+b}b^3},$$

$$c_3 = \frac{(-1+b)^{3/2}\sqrt{4-(2-\frac{2\sqrt{-1+b}e^{1-\frac{1}{\sqrt{-1+b}}}r}{b})^2}}{b},$$

$$c_4 = -\frac{(-4+b)(-1+b)^2e^2f\sqrt{4-(2-\frac{2\sqrt{-1+b}e^{1-\frac{1}{\sqrt{-1+b}}}r}{b})^2}}{2b^2},$$

$$d_1 = -\frac{2(-1+b)e^{-\frac{1}{\sqrt{-1+b}}}(\sqrt{-1+b}be^{\frac{1}{\sqrt{-1+b}}}+er-ber)}{b^2},$$

$$d_2 = \frac{(-4+b)(-1+b)^{3/2}e^{-\frac{1}{\sqrt{-1+b}}}(\sqrt{-1+b}be^{\frac{1}{\sqrt{-1+b}}}+er-ber)}{b^3},$$

$$d_3 = e^{1-\frac{2}{\sqrt{-1+b}}} r\bigg(2\sqrt{-1+b}b^3 e^{\frac{1}{\sqrt{-1+b}}} - 4er + b(-4\sqrt{-1+b}e^{\frac{1}{\sqrt{-1+b}}} + 6er)$$

$$+ b^2(2\sqrt{-1+b}e^{\frac{1}{\sqrt{-1+b}}} - (2+\sqrt{-1+b})er)\bigg) \Big/ \left(2\sqrt{-1+b}b^3\sqrt{\frac{e^{1-\frac{2}{\sqrt{-1+b}}} r(2\sqrt{-1+b}be^{\frac{1}{\sqrt{-1+b}}} + er - ber)}{b^2}}\right),$$

$$d_4 = -e^{1-\frac{2}{\sqrt{-1+b}}} r\bigg(24er + 6b(4\sqrt{-1+b}e^{\frac{1}{\sqrt{-1+b}}} - 7er) + 6b^4(\sqrt{-1+b}e^{\frac{1}{\sqrt{-1+b}}} - er)$$

$$+ b^2(-18\sqrt{-1+b}e^{\frac{1}{\sqrt{-1+b}}} + 6er) + b^3(-12\sqrt{-1+b}e^{\frac{1}{\sqrt{-1+b}}} + (19 - 3\sqrt{-1+b})er)\bigg)$$

$$\Big/ \left(6b^4\sqrt{\frac{e^{1-\frac{2}{\sqrt{-1+b}}} r(2\sqrt{-1+b}be^{\frac{1}{\sqrt{-1+b}}} + er - ber)}{b^2}}\right).$$

CONFLICT OF INTERESTS

The authors declare that there is no conflict of interests.

REFERENCES

[1] A.J. Lotka, Elements of physical biology, Science Progress in the Twentieth Century (1919-1933), 21 (1926), 341–343. http://www.jstor.org/stable/43430362.

[2] V. Volterra, Fluctuations in the abundance of a species considered mathematically, Nature. 118 (1926), 558–560. https://doi.org/10.1038/118558a0.

[3] Z. Ma, F. Chen, C. Wu, et al. Dynamic behaviors of a Lotka–Volterra predator–prey model incorporating a prey refuge and predator mutual interference, Appl. Math. Comput. 219 (2013), 7945–7953. https://doi.org/10.1016/j.amc.2013.02.033.

[4] A.A. Elsadany, A.E. Matouk, Dynamical behaviors of fractional-order Lotka-Volterra predator-prey model and its discretization, J. Appl. Math. Comput. 49 (2014), 269–283. https://doi.org/10.1007/s12190-014-0838-6.

[5] H. Deng, F. Chen, Z. Zhu, et al. Dynamic behaviors of Lotka-Volterra predator-prey model incorporating predator cannibalism, Adv. Differ. Equ. 2019 (2019), 359. https://doi.org/10.1186/s13662-019-2289-8.

[6] B. Xie, N. Zhang, Influence of fear effect on a Holling type III prey-predator system with the prey refuge, AIMS Math. 7 (2022), 1811–1830. https://doi.org/10.3934/math.2022104.

[7] A. Suleman, R. Ahmed, F.S. Alshammari, N.A. Shah, Dynamic complexity of a slow-fast predator-prey model with herd behavior, AIMS Math. 8 (2023), 24446–24472. https://doi.org/10.3934/math.20231247.

[8] A. Al Khabyah, R. Ahmed, M.S. Akram, et al. Stability, bifurcation, and chaos control in a discrete predator-prey model with strong Allee effect, AIMS Math. 8 (2023), 8060–8081. https://doi.org/10.3934/math.2023408.

[9] E. González-Olivares, J. Mena-Lorca, A. Rojas-Palma, et al. Dynamical complexities in the Leslie-Gower predator-prey model as consequences of the Allee effect on prey, Appl. Math. Model. 35 (2011), 366–381. https://doi.org/10.1016/j.apm.2010.07.001.

[10] M. Anacleto, C. Vidal, Dynamics of a delayed predator-prey model with Allee effect and Holling type II functional response, Math. Methods Appl. Sci. 43 (2020), 5708–5728. https://doi.org/10.1002/mma.6307.

[11] D. Sen, S. Ghorai, M. Banerjee, A. Morozov, Bifurcation analysis of the predator-prey model with the Allee effect in the predator, J. Math. Biol. 84 (2021), 7. https://doi.org/10.1007/s00285-021-01707-x.

[12] B. Mondal, S. Sarkar, U. Ghosh, Complex dynamics of a generalist predator-prey model with hunting cooperation in predator, Eur. Phys. J. Plus. 137 (2021), 43. https://doi.org/10.1140/epjp/s13360-021-02272-4.

[13] Y. Chou, Y. Chow, X. Hu, et al. A Ricker-type predator-prey system with hunting cooperation in discrete time, Math. Computers Simul. 190 (2021), 570–586. https://doi.org/10.1016/j.matcom.2021.06.003.

[14] M.Y. Hamada, T. El-Azab, H. El-Metwally, Allee effect in a Ricker type predator-prey model, J. Math. Computer Sci. 29 (2022), 239–251. https://doi.org/10.22436/jmcs.029.03.03.

[15] M.Y. Hamada, T. El-Azab, H. El-Metwally, Bifurcations and dynamics of a discrete predator-prey model of ricker type, J. Appl. Math. Comput. 69 (2022), 113–135. https://doi.org/10.1007/s12190-022-01737-8.

[16] C.S. Holling, Some characteristics of simple types of predation and parasitism, Canad. Entomol. 91 (1959), 385–398. https://doi.org/10.4039/ent91385-7.

[17] C. Arancibia-Ibarra, P. Aguirre, J. Flores, et al. Bifurcation analysis of a predator-prey model with predator intraspecific interactions and ratio-dependent functional response, Appl. Math. Comput. 402 (2021), 126152. https://doi.org/10.1016/j.amc.2021.126152.

[18] J.R. Beddington, Mutual interference between parasites or predators and its effect on searching efficiency, J. Animal Ecol. 44 (1975), 331–340. https://doi.org/10.2307/3866.

[19] D.L. DeAngelis, R.A. Goldstein, R.V. O'Neill, A model for tropic interaction, Ecology. 56 (1975), 881–892. https://doi.org/10.2307/1936298.

[20] P.H. Crowley, E.K. Martin, Functional responses and interference within and between year classes of a dragonfly population, J. North Amer. Benthol. Soc. 8 (1989), 211–221. https://doi.org/10.2307/1467324.

[21] P.A. Braza, Predator–prey dynamics with square root functional responses, Nonlinear Anal.: Real World Appl. 13 (2012), 1837–1843. https://doi.org/10.1016/j.nonrwa.2011.12.014.

[22] A.Q. Khan, I. Ahmad, H.S. Alayachi, et al. Discrete-time predator-prey model with flip bifurcation and chaos control, Math. Biosci. Eng. 17 (2020), 5944–5960. https://doi.org/10.3934/mbe.2020317.

[23] Z. AlSharawi, S. Pal, N. Pal, et al. A discrete-time model with non-monotonic functional response and strong Allee effect in prey, J. Differ. Equ. Appl. 26 (2020), 404–431. https://doi.org/10.1080/10236198.2020.1739276.

[24] R. Ahmed, A. Ahmad, N. Ali, Stability analysis and Neimark-Sacker bifurcation of a nonstandard finite difference scheme for Lotka-Volterra prey-predator model, Commun. Math. Biol. Neurosci. 2022 (2022), 61. https://doi.org/10.28919/cmbn/7534.

[25] A.Q. Khan, S.A.H. Bukhari, M.B. Almatrafi, Global dynamics, Neimark-Sacker bifurcation and hybrid control in a Leslie's prey-predator model, Alexandria Eng. J. 61 (2022), 11391–11404. https://doi.org/10.1016/j.aej.2022.04.042.

[26] M. Zhao, C. Li, J. Wang, Complex dynamic behaviors of a discrete-time predator-prey system, J. Appl. Anal. Comput. 7 (2017), 478–500. https://doi.org/10.11948/2017030.

[27] S.M.S. Rana, Dynamics and chaos control in a discrete-time ratio-dependent Holling-Tanner model, J. Egypt. Math. Soc. 27 (2019), 48. https://doi.org/10.1186/s42787-019-0055-4.

[28] P. Baydemir, H. Merdan, E. Karaoglu, et al. Complex dynamics of a discrete-time prey–predator system with Leslie type: stability, bifurcation analyses and chaos, Int. J. Bifurcation Chaos. 30 (2020), 2050149. https://doi.org/10.1142/s0218127420501497.

[29] S. Akhtar, R. Ahmed, M. Batool, et al. Stability, bifurcation and chaos control of a discretized Leslie prey-predator model, Chaos Solitons Fractals. 152 (2021), 111345. https://doi.org/10.1016/j.chaos.2021.111345.

[30] P.A. Naik, Z. Eskandari, H.E. Shahraki, Flip and generalized flip bifurcations of a two-dimensional discrete-time chemical model, Math. Model. Numer. Simul. Appl. 1 (2021), 95–101. https://doi.org/10.53391/mmnsa.2021.01.009.

[31] Z. Eskandari, Z. Avazzadeh, R.K. Ghaziani, et al. Dynamics and bifurcations of a discrete-time Lotka–Volterra model using nonstandard finite difference discretization method, Math. Methods Appl. Sci. (2022). https://doi.org/10.1002/mma.8859.

[32] P.A. Naik, Z. Eskandari, Z. Avazzadeh, et al. Multiple bifurcations of a discrete-time prey–predator model with mixed functional response, Int. J. Bifurcation Chaos. 32 (2022), 2250050. https://doi.org/10.1142/s021812742250050x.

[33] P.A. Naik, Z. Eskandari, A. Madzvamuse, et al. Complex dynamics of a discrete-time seasonally forced SIR epidemic model, Math. Methods Appl. Sci. 46 (2022), 7045–7059. https://doi.org/10.1002/mma.8955.

[34] W. Liu, D. Cai, Bifurcation, chaos analysis and control in a discrete-time predator-prey system, Adv. Differ. Equ. 2019 (2019), 11. https://doi.org/10.1186/s13662-019-1950-6.

[35] Y. Li, F. Zhang, X. Zhuo, Flip bifurcation of a discrete predator-prey model with modified Leslie-Gower and Holling-type III schemes, Math. Biosci. Eng. 17 (2020), 2003–2015. https://doi.org/10.3934/mbe.2020106.

[36] Rajni, B. Ghosh, Multistability, chaos and mean population density in a discrete-time predator-prey system, Chaos Solitons Fractals. 162 (2022), 112497. https://doi.org/10.1016/j.chaos.2022.112497.

[37] A.M. Yousef, A.M. Algelany, A.A. Elsadany, Codimension one and codimension two bifurcations in a discrete Kolmogorov type predator–prey model, J. Comput. Appl. Math. 428 (2023), 115171. https://doi.org/10.1016/j.cam.2023.115171.

[38] A.Q. Khan, I.M. Alsulami, Complicate dynamical analysis of a discrete predator-prey model with a prey refuge, AIMS Math. 8 (2023), 15035–15057. https://doi.org/10.3934/math.2023768.

[39] A. Tassaddiq, M.S. Shabbir, Q. Din, et al. Discretization, bifurcation, and control for a class of predator-prey interactions, Fractal Fract. 6 (2022), 31. https://doi.org/10.3390/fractalfract6010031.

[40] S. Lin, F. Chen, Z. Li, et al. Complex dynamic behaviors of a modified discrete Leslie-Gower predator–prey system with fear effect on prey species, Axioms. 11 (2022), 520. https://doi.org/10.3390/axioms11100520.

[41] P.A. Naik, Z. Eskandari, M. Yavuz, J. Zu, Complex dynamics of a discrete-time Bazykin-Berezovskaya prey-predator model with a strong Allee effect, J. Comput. Appl. Math. 413 (2022), 114401. https://doi.org/10.1016/j.cam.2022.114401.

[42] R. Ahmed, M. Rafaqat, I. Siddique, et al. Complex dynamics and chaos control of a discrete-time predator-prey model, Discr. Dyn. Nat. Soc. 2023 (2023), 8873611. https://doi.org/10.1155/2023/8873611.

[43] M.Y. Hamada, T. El-Azab, H. El-Metwally, Bifurcation analysis of a two-dimensional discrete-time predator–prey model, Math Methods Appl. Sci. 46 (2022), 4815–4833. https://doi.org/10.1002/mma.8807.

[44] D. Xiao, L.S. Jennings, Bifurcations of a ratio-dependent predator-prey system with constant rate harvesting, SIAM J. Appl. Math. 65 (2005), 737–753. https://doi.org/10.1137/s0036139903428719.

[45] R. Ahmed, Complex dynamics of a fractional-order predator-prey interaction with harvesting, Open J. Discret. Appl. Math. 3 (2020), 24–32. https://doi.org/10.30538/psrp-odam2020.0040.

[46] Q. Shu, J. Xie, Stability and bifurcation analysis of discrete predator–prey model with nonlinear prey harvesting and prey refuge, Math. Methods Appl. Sci. 45 (2021), 3589–3604. https://doi.org/10.1002/mma.8005.

[47] H.S. Panigoro, M. Rayungsari, A. Suryanto, Bifurcation and chaos in a discrete-time fractional-order logistic model with Allee effect and proportional harvesting, Int. J. Dyn. Control. 11 (2023), 1544–1558. https://doi.org/10.1007/s40435-022-01101-5.

[48] A.J. Kashyap, Q. Zhu, H.K. Sarmah, et al. Dynamical study of a predator-prey system with Michaelis-Menten type predator-harvesting, Int. J. Biomath. 16 (2022), 2250135. https://doi.org/10.1142/s1793524522501352.

[49] B. Mondal, S. Sarkar, U. Ghosh, An autonomous and nonautonomous predator–prey model with fear, refuge, and nonlinear harvesting: Backward, Bogdanov-Takens, transcritical bifurcations, and optimal control, Math. Methods Appl. Sci. 46 (2023), 17260–17287. https://doi.org/10.1002/mma.9499.

[50] W. Yao, X. Li, Complicate bifurcation behaviors of a discrete predator–prey model with group defense and nonlinear harvesting in prey, Appl. Anal. 102 (2022), 2567–2582. https://doi.org/10.1080/00036811.2022.2030724.

[51] X. Jia, M. Zhao, K. Huang, Bifurcation analysis and simulations of a modified Leslie-Gower predator-prey model with constant-type prey harvesting, Math. Methods Appl. Sci. 46 (2023), 18789–18814. https://doi.org/10.1002/mma.9593.

[52] A. Singh, V.S. Sharma, Codimension-2 bifurcation in a discrete predator–prey system with constant yield predator harvesting, Int. J. Biomath. 16 (2022), 2250109. https://doi.org/10.1142/s1793524522501091.

[53] S. Marick, S. Bhattacharya, N. Bairagi, Dynamic properties of a reaction-diffusion predator-prey model with nonlinear harvesting: A linear and weakly nonlinear analysis, Chaos Solitons Fractals. 175 (2023), 113996. https://doi.org/10.1016/j.chaos.2023.113996.

[54] M.B. Almatrafi, M. Berkal, Bifurcation analysis and chaos control for prey-predator model with Allee effect, Int. J. Anal. Appl. 21 (2023), 131. https://doi.org/10.28924/2291-8639-21-2023-131.

[55] R. Ahmed, M.B. Almatrafi, Complex dynamics of a predator-prey system with Gompertz growth and herd behavior, Int. J. Anal. Appl. 21 (2023), 100. https://doi.org/10.28924/2291-8639-21-2023-100.

[56] M. Berkal, M.B. Almatrafi, Bifurcation and stability of two-dimensional activator–inhibitor model with fractional-order derivative, Fractal Fract. 7 (2023), 344. https://doi.org/10.3390/fractalfract7050344.

[57] A.Q. Khan, M.B. Almatrafi, Two-dimensional discrete-time laser model with chaos and bifurcations, AIMS Math. 8 (2023), 6804–6828. https://doi.org/10.3934/math.2023346.

[58] A.Q. Khan, F. Nazir, M.B. Almatrafi, Bifurcation analysis of a discrete Phytoplankton-Zooplankton model with linear predational response function and toxic substance distribution, Int. J. Biomath. 16 (2022), 2250095. https://doi.org/10.1142/s1793524522500954.

[59] A.C.J. Luo, Regularity and complexity in dynamical systems, Springer, New York, 2012. https://doi.org/10.1007/978-1-4614-1524-4.

[60] J. Guckenheimer, P. Holmes, Nonlinear oscillations, dynamical systems, and bifurcations of vector fields, Springer, New York, 1983. https://doi.org/10.1007/978-1-4612-1140-2.

[61] S. Wiggins, M. Golubitsky, Introduction to applied nonlinear dynamical systems and chaos, Springer, New York, 2003. https://doi.org/10.1007/b97481.

[62] G. Chen, X. Dong, From chaos to order: methodologies, perspectives and applications, World Scientific, 1998. https://doi.org/10.1142/3033.

[63] C. Lei, X. Han, W. Wang, Bifurcation analysis and chaos control of a discrete-time prey-predator model with fear factor, Math. Biosci. Eng. 19 (2022), 6659–6679. https://doi.org/10.3934/mbe.2022313.

[64] X.S. Luo, G. Chen, B.H. Wang, et al. Hybrid control of period-doubling bifurcation and chaos in discrete nonlinear dynamical systems, Chaos Solitons Fractals. 18 (2003), 775–783. https://doi.org/10.1016/s0960-0779(03)00028-6.